

Magnetic functionality of thin film perovskite hybrids

Aisha Aqeel, Naureen Akhtar, Alexey O. Polyakov, Petra Rudolf, Thomas T. M. Palstra

Angaben zur Veröffentlichung / Publication details:

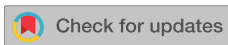
Aqeel, Aisha, Naureen Akhtar, Alexey O. Polyakov, Petra Rudolf, and Thomas T. M. Palstra. 2018. "Magnetic functionality of thin film perovskite hybrids." *APL Materials* 6 (11): 114206. <https://doi.org/10.1063/1.5042323>.

RESEARCH ARTICLE | NOVEMBER 16 2018

Magnetic functionality of thin film perovskite hybrids

Special Collection: [2D Hybrid Organic-Inorganic Perovskites](#)

Aisha Aqeel; Naureen Akhtar; Alexey O. Polyakov; Petra Rudolf; Thomas T. M. Palstra 




APL Mater. 6, 114206 (2018)

<https://doi.org/10.1063/1.5042323>




CrossMark



Special Topic: Ultrafast Materials Science: Coherence and Dynamics

Submit Today!



Magnetic functionality of thin film perovskite hybrids

Aisha Aqeel,^{1,2} Naureen Akhtar,^{2,3} Alexey O. Polyakov,² Petra Rudolf,² and Thomas T. M. Palstra^{2,a}

¹Department of Physics, University of Regensburg, Regensburg 93053, Germany

²Zernike Institute for Advanced Materials, University of Groningen, Nijenborgh 4, NL-9747AG Groningen, The Netherlands

³Department of Physics and Technology, University of Bergen, P.O. Box 7803, N-5020 Bergen, Norway

(Received 31 May 2018; accepted 28 September 2018; published online 16 November 2018)

Organic-inorganic perovskite-like hybrids combine the properties of both the perovskite structure and metal-organic framework compounds. We investigated the magnetic properties of a Cu-based hybrid material grown as a thin film by the Langmuir-Blodgett technique. We show that the long alkyl spacers in the hybrid thin film only slightly reduce the ferromagnetic transition temperature in comparison with the bulk. Most interestingly, the single ion anisotropy is larger for the Cu-based hybrid film than for the bulk hybrid. The hybrid thin film consists of two polymorphs in which the ferromagnetic domains are effectively pinned by an antiferromagnetic phase. This leads to a large enhancement of the coercive field enabling memory functionality. © 2018 Author(s). All article content, except where otherwise noted, is licensed under a Creative Commons Attribution (CC BY) license (<http://creativecommons.org/licenses/by/4.0/>). <https://doi.org/10.1063/1.5042323>

Layered crystal structures are present in a rich variety of materials with properties including topological surface states,¹ superconductivity,^{2,3} ferroelectricity,⁴ and colossal magnetoresistance.⁵ One of the most interesting and promising classes in this family situates itself at the boundary between the perovskite materials and metal-organic frameworks (MOFs) and comprises layered organic-inorganic perovskite-like hybrids.^{6–9} These compounds combine the robust functional properties of inorganic perovskites with the structurally versatile organization of MOFs, creating a remarkable merger. Extensive studies over the last years revealed that these organic-inorganic hybrids exhibit ferromagnetism,^{10–12} photovoltaic properties,^{13,14} and multiferroicity.^{15,16} Perovskite-like organic-inorganic hybrids generally consist of two- and three-dimensional systems, depending on how the inorganic blocks are connected and related to the size of organic components and halogens. Easy processing from solution and structural flexibility make these hybrids promising candidates for tailoring and optimizing these properties, also exploiting the different dimensionalities. Two-dimensional hybrids consist of inorganic sheets, formed by corner-shared MX₆ octahedra and intercalated by layers of the organic components.⁶ The organic part is often connected to the inorganic part by hydrogen bonds via NH₃ groups. Multiferroicity, i.e., coexistence of ferromagnetism and ferroelectricity, was discovered in the hybrid CuCl₄(C₆H₅CH₂CH₂NH₃)₂ (hereafter CuCl₄(PEA))₂.¹⁵ The ferromagnetism originates from the inorganic part, while the relative importance of the mechanism for ferroelectricity is still under debate: both rotational order arising from the NH₃ group¹⁵ and displacive order¹⁷ originating from the dipole moment of the A-group cation¹⁶ have been shown to contribute. The present manuscript focuses on the magnetic functionality of a CuCl₄-based organic-inorganic hybrid Langmuir-Blodgett (LB) film.

In organic-inorganic hybrids, magnetism originates from the transition metal ions in the perovskite-like sheets.¹⁰ Neighbouring ions interact antiferromagnetically in-plane in the case of Mn- or Fe-based hybrids, via a 180° superexchange path involving the bridging Cl ions.^{18,19} However, in the case of Cu²⁺ s = 1/2-based hybrids, the CuCl₆ octahedra are distorted due to a

^aElectronic mail: t.t.m.palstra@utwente.nl

collective Jahn-Teller distortion.^{11,15,20} The in-plane elongation of the CuCl_6 octahedra shows that the magnetic spin originates from the unoccupied $\text{Cu } dx^2 - y^2$ orbital. In this case, the $dx^2 - y^2$ type symmetry orbitals of the individual Cu ions in the a-b basal plane are orthogonal to each other.²⁰ Such an orbital arrangement leads to ferromagnetic (FM) coupling between the Cu ions. The ferromagnetic coupling in-plane leads to the in-plane 2D order and an apparent quasi-3D ferromagnetic ordering; in fact, the well-known Cu-based hybrid $\text{CuCl}_4(\text{PEA})_2$ behaves as a Heisenberg ferromagnet.¹⁵ In the Cu-based hybrid LB film, the same inorganic structural arrangement is expected.²¹ A good example of a double-layered perovskite is $\text{K}_3\text{Cu}_2\text{F}_7$ ²²—in this compound a collective Jahn-Teller distortion is also present, leading to ferromagnetic (FM) interactions between Cu ions in-plane. However, in the out-of-plane direction, the Cu-ions couple antiferromagnetically through a super-exchange pathway via bridging fluorine atoms.²³ We expect the same antiferromagnetic (AF) structure for the hybrid LB film if there is a similarity in the crystal structure.

We used the LB technique^{24,25} to synthesize CuCl_4 -based organic-inorganic thin films.^{21,26,27} CuCl_4 -based hybrid films were prepared on non-magnetic substrates from a chloroform-methanol and octadecyl ammonium chloride ($\text{ODAH}^+ \text{Cl}^-$) solution spread onto a subphase. The subphase contained an aqueous solution of copper chloride (CuCl_2) and methyl ammonium chloride. First, the subphase was slowly compressed with a movable barrier into octahedral organic-inorganic sheets in which the octahedras containing six Cl atoms, 4 atoms sharing neighbouring atoms in-plane, one from the ODAH^+Cl^- molecule, and the last from the methyl ammonium chloride, encage the Cu^{+2} ions at the centre. These compressed organic-inorganic sheets were deposited layer-by-layer onto hydrophobic substrates by vertical dipping of the substrates into the subphase. The film adopts a different crystal structure than the bulk crystals. In the bulk crystals, the CuCl_4 layers are coordinated on both sides by the same components.^{6,7,15} The use of LB implies an alternation of hydrophilic and hydrophobic end groups during the deposition: octadecylamine (ODA) and methylamine (MA) with CuCl_2 as the inorganic precursor.²¹ The presence of inorganic CuCl_4 -based backbone structure in LB films was confirmed by X-ray photoelectron spectroscopy.

X-ray diffraction data (not shown here) demonstrate high quality growth of the CuCl_4 -based organic-inorganic LB films with the full width at half maximum of the rocking curve less than 0.04° . As clearly seen in the scanning electron micrograph shown in Fig. 1, the LB hybrid film consists of two phases with different Cu:Cl ratios.²¹ The main phase ($\sim 70\%$) has a Cu:Cl ratio of 1:4; the CuCl_4 layer is sandwiched between hydrophilic MA on one side and ODA on the other side, providing a hydrophobic termination. MA is so small that it allows ionic coupling between the two adjacent Cu–Cl layers, analogous to alkali (earth) ions in perovskites [Fig. 1 (left)]. The inorganic part of the main thin film phase is therefore structurally similar to the classical bulk perovskite-like hybrids:^{22,28} one inorganic layer intercalated by organic components. The second phase (30%), with a Cu:Cl ratio of 1:3, can be ascribed²¹ to a Cu–Cl double layer perovskite hybrid in analogy with $\text{K}_3\text{Cu}_2\text{F}_7$.²² In this case, the inorganic layers share apical Cl atoms [Fig. 1 (right)] and the MA components occupy the icosahedral cavities between the octahedra.²¹

To measure the magnetic properties of a LB film in a conventional magnetometer, a relatively thick film needed to be deposited on a suitable non-magnetic substrate to obtain a sufficient signal/noise ratio. We therefore deposited 1184 layers of the hybrid film on a glass substrate. Magnetization

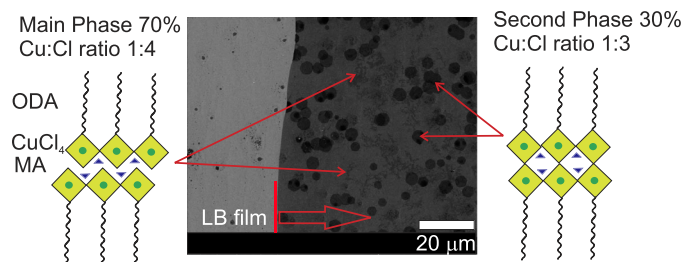


FIG. 1. SEM micrograph of a 3-layer-thick CuCl_4 -based organic-inorganic thin film grown by Langmuir-Blodgett deposition: the micrograph reveals the presence of a second phase (right), which exhibits a different layering scheme than the template-induced main phase (left). Figure adapted from Ref. 21.

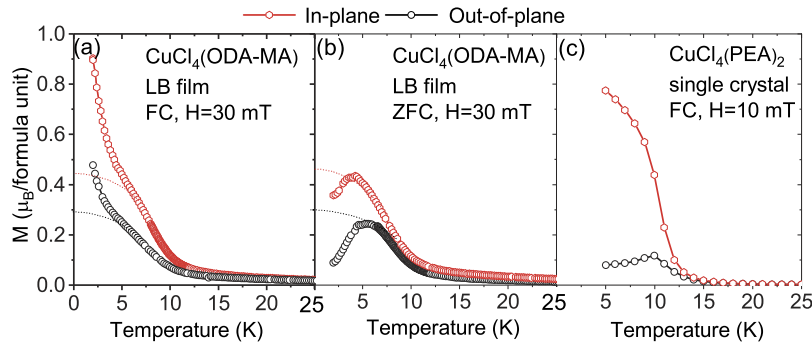


FIG. 2. (a) Field cooled (FC) and (b) zero field cooled (ZFC) magnetization versus temperature measured in 30 mT for a 1184-layer-thick CuCl_4 -based hybrid film grown by Langmuir-Blodgett deposition, measured in-plane (red) and out-of-plane (black). The dotted lines in (a) and (b) serve as guidelines to the estimated spontaneous magnetization at $T = 0$ K. (c) In-plane and out-of-plane measurements for the bulk hybrid $\text{CuCl}_4(\text{PEA})_2$, adapted from Ref. 15.

measurements were performed with a Quantum Design SQUID XL magnetometer. The sample was mounted in a gelatin capsule, fixed in a plastic straw. In the following, we shall discuss that the magnetic order is remarkably robust to this asymmetric coordination despite the long intercalating groups and the different anisotropy; we shall also show the influence of the second phase on the magnetic coercivity.

Field cooled [FC, Fig. 2(a)] measurements in a 1 T magnetic field and zero field cooled [ZFC, Fig. 2(b)] measurements were performed with the in-plane and out-of-plane applied field. The applied magnetic field strength H is defined in SI units as $\mu_0 H$ throughout the paper. The data testify to ferro-magnetic ordering below $T_c = 8.2$ K where the FC and ZFC measurements deviate from each other.

The anisotropy of the magnetization in thin films is less pronounced than for bulk samples. In the single crystalline bulk hybrid $\text{CuCl}_4(\text{PEA})_2$, the magnetic easy axis is in-plane [Fig. 2(c)]. The in-plane thin film magnetization data can be fitted in the temperature region above T_c by a Curie-Weiss law with a Curie constant $C = 0.431 \pm 0.003$ emu K/mol and a Weiss temperature $\theta = 3.20 \pm 0.01$ K. The in-plane Curie constant is close to that observed in the bulk hybrid $\text{CuCl}_4(\text{PEA})_2$, where $C = 0.360 \pm 0.001$ emu K/mol. The Curie constant for the film in the out-of-plane measurement direction is $C = 0.652 \pm 0.003$ emu K/mol and $\theta = 6.80 \pm 0.01$ K. Figure 3 shows the $M(H)$ curves for the Cu-based hybrid film; the measurements for bulk crystals are shown in Fig. 4 as a reference. The large anisotropy below T_c observed for the single crystalline bulk sample is much reduced for the LB film. The film shows a hysteresis loop with a remnant magnetization of 3.1 emu/mm² and a coercive field $H_c \approx 27$ mT [Fig. 3(d)] for H in-plane at 3 K. Also, the magnetization does not saturate but increases linearly at high fields [Fig. 3(a)]. This indicates a contribution from the additional

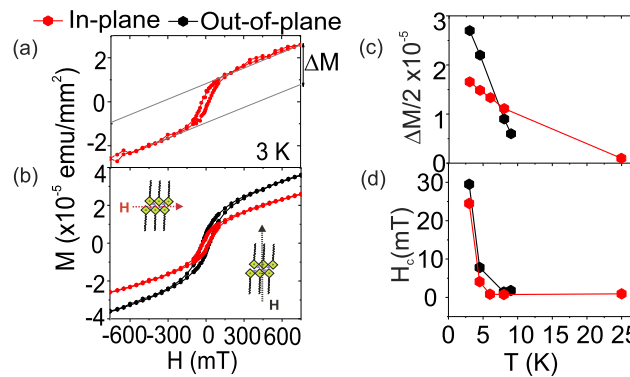


FIG. 3. Magnetic hysteresis loops for a 1184-layer-thick CuCl_4 -based organic-inorganic thin film grown by Langmuir-Blodgett deposition and measured (a) in-plane and (b) both in-plane and out-of-plane at 5 K. (c) and (d) show ΔM [defined in Fig. 3(a)] and the coercive field H_c as a function of temperature, respectively.

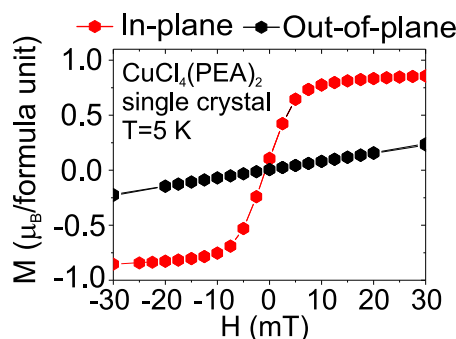


FIG. 4. Magnetization versus externally applied magnetic field H at 5 K for a $\text{CuCl}_4(\text{PEA})_2$ crystal measured in the in-plane and out-of-plane configurations, adapted from Ref. 15.

antiferromagnetic component. The magnetization curves at 3 K for the in-plane and out-of-plane geometries [Fig. 3(b)] show the existence of much enhanced coercive fields in the hybrid LB film, as compared to the bulk crystal.

The bulk $\text{CuCl}_4(\text{PEA})_2$ hybrid is ferromagnetic with $T_c = 11$ K. The different layer structure of the hybrid film implies changes in the single ion anisotropy of the Cu^{2+} ions, which is determined by the coordination and should therefore be similar below and above T_c .²⁹ On the other hand, the shape anisotropy influences the magnetism only below T_c . The hybrid bulk compound shows $M(T)$ curves that resemble a classical Heisenberg ferromagnet, with the same values of the in-plane and out-of-plane Curie constants ($C_{\text{bulk}} = 0.36$ emu K/mol).³⁰ For the CuCl_4 -based hybrid LB film, the difference between the in-plane ($C_{\text{in-plane}} = 0.49$ emu K/mol) and out-of-plane ($C_{\text{out-of-plane}} = 0.65$ emu K/mol) Curie constants indicates a larger single ion anisotropy than in the bulk hybrid. This is attributed to the asymmetric coordination of the CuCl_6 octahedra, since the MA and ODA components alternate [Fig. 1 (left)] in the thin films.

For the CuCl_4 -based hybrid LB film, $M(T)$ decreases more rapidly near T_c , pointing to larger fluctuations, possibly related to a lower T_c and to a smaller magnetic domain size. The spontaneous magnetization for the CuCl_4 -based hybrid LB film is defined by extrapolation of the maximum of the $M(T)$ curve to $T = 0$ K without considering the low temperature (3 K–4 K) paramagnetic tail appearing in the FC magnetization curves [see Fig. 2(a)]. The estimated spontaneous magnetization amounts to an in-plane value of $\sim 0.45 \pm 0.04 \mu_B/\text{Cu}$ and an out-of-plane value of $\sim 0.29 \pm 0.04 \mu_B/\text{Cu}$ [indicated by dotted lines in Figs. 2(a) and 2(b)]. These values are significantly smaller than the $0.8 \mu_B/\text{Cu}$ in-plane value for the bulk $\text{CuCl}_4(\text{PEA})_2$ hybrid [Fig. 2(c)]. The ZFC curves for the CuCl_4 -based hybrid LB film [Figs. 2(a) and 2(b)] clearly indicate that the easy axis is in-plane. This is evident from the fact that the ZFC out-of-plane magnetization extrapolates to $M = 0$ at $T = 0$ K [Fig. 2(b)]; also, the in-plane magnetization is not temperature dependent below T_c .

The $M(H)$ curves of the hybrid LB film do not saturate at high field (Fig. 3). We ascribe this to an antiferromagnetic (AF) contribution of the second phase, which, as indicated by XPS and SEM, makes up $\sim 30\%$ of the sample.²¹ We propose that the different type of inorganic layering defines the magnetic behaviour of the second phase where the Cu:Cl ratio amounts to 1:3 and the inorganic block is formed by double-perovskite-like Cu_2Cl_7 layers with shared apical chlorine atoms. In this phase, the Cu ions exhibit AF super-exchange interactions in the out-of-plane direction via bridging apical chlorine ions, similarly to the double-layer perovskite $\text{K}_3\text{Cu}_2\text{F}_7$.²² However, the in-plane magnetic interaction for the second phase remains FM. This is supported by the fact that the slope of the $M(H)$ curves at $H \gg H_c$ for the out-of-plane measurement is larger than that in the bulk [cf. Figs. 3(b) and 3(c) with Fig. 4]. An important property of the hybrid film is the presence of a finite coercive field, which has never been observed for Cu-based bulk hybrids. We propose that the finite coercive field arises due to pinning of the domain walls on the inclusions of the second phase (see the SEM image in Fig. 1); however, this requires an in-depth study which is beyond the scope of this paper.

The transition temperature (T_c) of the ferromagnetic transition for the hybrid LB film can be determined by plotting the derivative of the zero-field cooled (ZFC) magnetization, $dM_{\text{ZFC}}(T)/dT$, versus temperature. Figure 5 shows dM/dT measured in various fields for the in-plane and

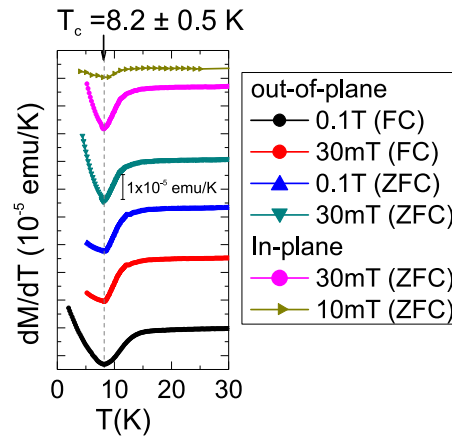


FIG. 5. First derivative of the magnetization vs. temperature plotted for the in-plane (IP) and the out-of-plane (OP) configurations, measured in field cooled (FC) and zero field cooled (ZFC) modes at different fields for a 1184-layer-thick CuCl_4 -based hybrid LB film.

out-of-plane configurations. The transition temperature, defined as the inflection point of dM/dT versus T , is $T_c = 8.2 \pm 0.5$ K. This value of T_c is the same for both the in-plane and the out-of-plane configurations.

Let us now consider the critical behaviour of our system that undergoes a second order phase transition at $T_c = 8.2$ K. Various critical exponents can be identified: below T_c , the spontaneous magnetization varies with $(T-T_c)^\beta$; above T_c , the initial susceptibility varies with $(T-T_c)^\gamma$, while $M/H \sim (T-T_c)^\delta$ at $T = T_c$. For the out-of-plane magnetization of the film, the critical exponent values are found to be $\beta = 0.280 \pm 0.006$ [Fig. 6(a)], $\gamma = 0.883 \pm 0.002$ [Fig. 6(b)], and $\delta = 3.84 \pm 0.1$ [Fig. 6(c)].

The value of the critical exponent β is lower than what is predicted for traditional 3D Heisenberg ferromagnets³¹ but close to the prediction by Pearce and Kim, using 2D conformal theory related to a hard squares (hexagon) model of continually varying exponents,³¹ for a similar magnetic system. This behaviour can be related to the quasi two-dimensional nature of the ferromagnetic system.

The behaviour of low-dimensional magnetic systems is governed by the Mermin-Wagner theorem.³² According to this theorem, the (anti)ferromagnetism should not occur in low-dimensional systems³² due to the absence of spontaneous symmetry breaking and that long-range order is destroyed by thermal fluctuations. In contrary to this theorem, long-range ferromagnetic order has been observed in nearly ideal $S = 1/2$, 2D Heisenberg CuCl_4 -based bulk hybrids.¹⁵ This can be the result of a finite anisotropy in the interlayer and intralayer exchange interactions. For these crystals, the intralayer exchange constant J is strong due to the cooperative Jahn-Teller ordering leading to ferromagnetic coupling, while the interlayer exchange constant \tilde{J} is very weak: $|\tilde{J}/J| \leq 10^{-3}$ and it defines the overall 3D character of the compounds.²⁹ The presence of interlayer exchange breaks the 2D character or axial magnetic anisotropy¹¹ H^{Ising} . Both ferromagnetic and antiferromagnetic interlayer interactions are possible, depending on the variations between J and H^{Ising} . Like bulk hybrid crystals, the CuCl_4 -based hybrid LB films are also observed to have long-range ferromagnetic order as discussed above.

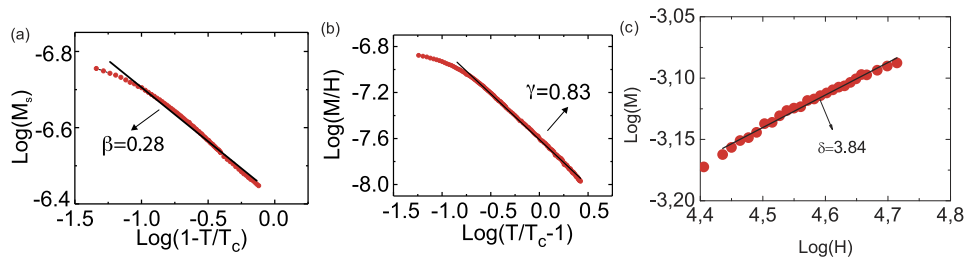


FIG. 6. (a) $\text{Log}(M_s)$ vs. $\text{log}(1-T/T_c)$, (b) $\text{log}(M/H)$ vs. $\text{log}(T/T_c-1)$, and (c) $\text{log}(M)$ versus $\text{log}(H)$ for $T_c = 8.2$ K for a 1184-layer-thick Cu-based hybrid LB film.

In these hybrid LB films, the observed Curie constants for in-plane and out-of-plane magnetization configurations differ even less than 20%. This indicates the presence of a Heisenberg spin. The observed critical exponents for both in-plane and out of plane measurements also point to a quasi-2D-Heisenberg system. In quasi-2D Heisenberg ferromagnets, the anisotropies lead to a deviation from the ideal 2D behaviour with a finite transition temperature related to the long-range order as discussed above.

In conclusion, the epitaxy between the organic and inorganic layers can be accommodated in Langmuir-Blodgett films with long alkyl chains, in contrast to the more soluble, shorter organic blocks in bulk crystals. The Cu^{2+} ions in LB films have an octahedral chlorine coordination, similar to the CuCl_4 -based bulk compounds. This results in perovskite-like sheets of CuCl_4 . Nevertheless, important differences in the magnetic properties occur due to the introduction of alternating MA and ODA organic component layers in the LB growth. The different layering gives rise to a significantly modified single ion anisotropy. Also, pinning of the ferromagnetic domains by the antiferromagnetic second phase gives rise to a large coercive field in the hybrid film. These properties are relevant in order to control and change the preferred direction of the magnetization as well as the anisotropy of the hybrid materials. The tailored layer-by-layer synthesis of CuCl_4 -based hybrid films paves the way for a new family of ferromagnetic thin films.

This work was performed within the “Top Research School” program of the Zernike Institute for Advanced Materials under the Bonus Incentive Scheme (BIS) of the Netherlands’ Ministry of Education, Science, and Culture.

- ¹ C. L. Kane and E. J. Mele, *Phys. Rev. Lett.* **95**, 146802 (2005).
- ² Y. Kamihara, T. Watanabe, M. Hirano, and H. Hosono, *J. Am. Chem. Soc.* **130**, 3296 (2008).
- ³ T. Watanabe, H. Yanagi, T. Kamiya, Y. Kamihara, H. Hiramatsu, M. Hirano, and H. Hosono, *Inorg. Chem.* **46**, 7719 (2007).
- ⁴ K. Kimura, H. Nakamura, S. Kimura, M. Hagiwara, and T. Kimura, *Phys. Rev. Lett.* **103**, 107201 (2009).
- ⁵ C. N. R. Rao, A. K. Cheetham, and R. Mahesh, *Chem. Mater.* **8**, 2421 (1996).
- ⁶ D. B. Mitzi, *J. Chem. Soc., Dalton Trans.* **2001**, 1.
- ⁷ D. B. Mitzi, C. D. Dimitrakopoulos, and L. L. Kosbar, *Chem. Mater.* **13**, 3728 (2001).
- ⁸ C. R. Kagan, D. B. Mitzi, and C. D. Dimitrakopoulos, *Science* **286**, 945 (1999).
- ⁹ A. H. Arkenbout, T. Uemura, J. Takeya, and T. T. M. Palstra, *Appl. Phys. Lett.* **95**, 173104 (2009).
- ¹⁰ W. E. Estes, D. B. Losee, and W. E. Hatfield, *J. Chem. Phys.* **72**, 630 (1980).
- ¹¹ L. D. Jongh, W. V. Amstel, and A. Miedema, *Physica* **58**, 277 (1972).
- ¹² P. Rabu and M. Drillon, *Adv. Eng. Mater.* **5**, 189 (2003).
- ¹³ M. A. Loi and J. C. Hummelen, *Nat. Mater.* **12**, 1087 (2013).
- ¹⁴ J. H. Heo, S. H. Im, J. H. Noh, T. N. Mandal, C.-S. Lim, J. A. Chang, Y. H. Lee, H.-j. Kim, A. Sarkar, Md. K. Nazeeruddin, M. Gratzel, and S. I. Seok, *Nat. Photonics* **7**, 486 (2013).
- ¹⁵ A. O. Polyakov, A. H. Arkenbout, J. Baas, G. R. Blake, A. Meetsma, A. Caretta, P. H. M. van Loosdrecht, and T. T. M. Palstra, *Chem. Mater.* **24**, 133 (2012).
- ¹⁶ D. Di Sante, A. Stroppa, P. Jain, and S. Picozzi, *J. Am. Chem. Soc.* **135**, 18126 (2013).
- ¹⁷ A. Caretta, R. Miranti, R. W. A. Havenith, E. Rampi, M. C. Donker, G. R. Blake, M. Montagnese, A. O. Polyakov, R. Broer, T. T. M. Palstra, and P. H. M. van Loosdrecht, *Phys. Rev. B* **89**, 024301 (2014).
- ¹⁸ M. A. Ahmed, M. A. Mousa, and F. A. Radwan, *J. Mater. Sci.* **23**, 4345 (1988).
- ¹⁹ R. Willett and E. Riedel, *Chem. Phys.* **8**, 112 (1975).
- ²⁰ D. Khomskii and K. Kugel, *Solid State Commun.* **13**, 763 (1973).
- ²¹ N. Akhtar, A. O. Polyakov, A. Aqeel, P. Gordiichuk, G. R. Blake, J. Baas, H. Amenitsch, A. Herrmann, P. Rudolf, and T. T. M. Palstra, *Small* **10**, 4912 (2014).
- ²² H. Manaka, Y. Miyashita, Y. Watanabe, and T. Masuda, *J. Phys. Soc. Jpn.* **76**, 085003 (2007).
- ²³ W. Brzezicki and A. M. Oleś, *J. Phys.: Conf. Ser.* **391**, 012085 (2012).
- ²⁴ H. Sugai, T. Iijima, and H. Masumoto, *Jpn. J. Appl. Phys., Part 1* **38**, 5322 (1999).
- ²⁵ M. Clemente-León, E. Coronado, A. Soriano-Portillo, E. Colacio, J. M. Domínguez-Vera, N. Gálvez, R. Madueño, and M. T. Martín-Romero, *Langmuir* **22**, 6993 (2006).
- ²⁶ N. Akhtar, G. R. Blake, R. Felici, H. Amenitsch, T. T. M. Palstra, and P. Rudolf, *Nano Res.* **7**, 1832 (2014).
- ²⁷ J. Wu, N. Akhtar, R. Y. N. Gengler, T. T. M. Palstra, and P. Rudolf, *J. Mater. Chem. C* **5**, 1782 (2017).
- ²⁸ B. Sachs, T. O. Wehling, K. S. Novoselov, A. I. Lichtenstein, and M. I. Katsnelson, *Phys. Rev. B* **88**, 201402 (2013).
- ²⁹ L. J. D. Jongh and A. R. Miedema, *Adv. Phys.* **50**, 947 (2001).
- ³⁰ A. H. Arkenbout, Zernike Institute PhD thesis series 2010-13, ISSN 1570-1530, ISBN: 978-90-367-4515-4, 2010.
- ³¹ P. A. Pearce and D. Kim, *J. Phys. A: Math. Gen.* **20**, 6471 (1987).
- ³² N. D. Mermin and H. Wagner, *Phys. Rev. Lett.* **17**, 1133 (1966).